NON-INDUCTIVE CURRENT DRIVE*

Egbert Westerhof

FOM Institute DIFFER, Dutch Institute for Fundamental Energy Research,
PO Box 6336, 5600 HH Eindhoven, The Netherlands, www.differ.nl

* These lecture notes are identical (except for minor corrections) to the lecture notes appearing in the proceedings of the 10th Carolus Magnus Summer School

ABSTRACT

This lecture addresses the various ways of non-inductive current generation. In particular, the topics covered include the bootstrap current, RF current drive, neutral beam current drive, alternative methods, and possible synergies between different ways of non-inductive current generation.

I. INTRODUCTION

Earlier lectures [1,2] have stressed the requirement of a finite poloidal magnetic field in addition to the toroidal magnetic field in order to confine charged particles in a toroidal configuration. Whereas in a stellarator the poloidal field is supplied by external coils [3], the tokamak relies on a toroidal plasma current for the generation of the poloidal field. Generally, the toroidal current in a tokamak is generated inductively by means of a transformer, in which the plasma acts as the secondary winding [1]. This immediately leads to a major limitation of tokamak operation: the finite flux swing of the transformer in combination with the finite resistivity of the plasma results in a finite pulse length of a tokamak discharge and necessarily pulsed reactor operation. For many reasons steady state operation of a fusion reactor is highly desirable. This has motivated the development of alternate ways for the generation of the toroidal plasma current. Such methods are classified as 'non-inductive current drive'. A second advantage offered by non-inductive current drive, is that it decouples the current density profile from the temperature profile, which determines the plasma conductivity and consequently defines the inductive current density profile. The freedom to shape the current density profile is particularly important for the control of plasma stability [4, 5].

An important measure is the efficiency of current drive which can be defined as the ratio of the driven current density, j, over the spent power density, p: $\gamma_{CD} \equiv j/p$. Since the total current generated scales as $I_{CD} \sim \pi a^2 j$, while the total spent power scales as $P \sim 2\pi R \pi a^2 p$, a more practical measure for the current drive efficiency is $\eta_{CD} \equiv n_e R I_{CD}/P$. Here, a and R are the minor and major radius of the tokamak, respectively. The factor n_e accounts for the fact that in many cases the non-inductively driven current is inversely proportional to the density such that the current drive efficiency η_{CD} becomes a constant which can be compared across different experiments and used for extrapolation to future devices.

Subsequent sections treat various methods of non-inductive current generation. First, the so-called bootstrap current is discussed, which in a toroidal device comes entirely for free. It is a parallel (with respect to the magnetic field) plasma current which is driven by finite pressure gradients in toroidal geometry. Next, the various methods of non-inductive current generation by radio frequency (RF) waves are treated. This is followed by a discussion of the current generated by injection of neutral particle beams and a brief overview of various alternate concepts for non-inductive current generation.

For further reading we advice the excellent early review by N.J. Fisch [6], and for later updates the relevant chapters of the ITER Physics Basis [7] and its update [8]. Very instructive is also the book by J. Wesson [9].

II. BOOTSTRAP CURRENT

Neoclassical, collisional transport [10] in high pressure toroidal plasma generates a finite parallel plasma current. This current is known as the bootstrap current and is entirely self generated by the plasma [9, 11]. Its origin can be best understood as follows. In toroidal plasma the particles do not follow the magnetic field lines exactly, but exhibit a finite drift as a consequence of the magnetic field curvature and inhomogeneity. For the trapped particles this results in banana shaped orbits with a finite width [4]

$$w_b = 2\frac{mv_{\|,m}}{qB_{p,m}}, \qquad (1)$$

where q is the charge of the particle, m its mass, and $v_{\|,m}$ and $B_{p,m}$ are the parallel velocity and poloidal magnetic field at the mid plane (i.e. the position of minimum magnetic field along the orbit). In the presence of a finite density gradient, this results at any given point on the mid plane in an imbalance between the trapped particles moving in co- and counter-current direction. This constitutes the banana current. The bootstrap current finally is generated through collisional coupling of the trapped and passing particles. Formulated in terms of the velocity distribution function at a given position on the

low field side of the mid plane, one notices that a finite density gradient results in an asymmetry in the trapped particle region. Collisions will extend this asymmetry across the trapped passing boundary into the passing particle region resulting in the bootstrap current.
In a more complete theory, not only the density gradient, but also the temperature gradient is seen to contribute to the bootstrap current. For large aspect ratio $\varepsilon^{-1} \equiv R/a$, the expression for the bootstrap current is [10]

$$j_{BS} = -\frac{\sqrt{\varepsilon} n}{B_p}\left(2.44(T_e + T_i)\frac{dn}{ndr} + 0.69\frac{dT_e}{dr} - 0.42\frac{dT_i}{dr} \right), \tag{2}$$

while for $\varepsilon \to 1$ it reduces to [10]

$$j_{BS} = -\frac{1}{B_p}\frac{dp}{dr}, \tag{3}$$

where p is the total plasma pressure.

III. PRINCIPLES OF RF CURRENT DRIVE [6]

Intuitively, the generation of a non-inductive current appears to require some method to directly impart parallel momentum to electrons. This could be done for example by means of neutral beams (see Section IV) or through resonant interaction with RF waves. In the latter case, the wave can impart its energy and momentum to electrons satisfying either the Landau resonance, $\omega - \boldsymbol{k}\cdot\boldsymbol{v} = 0$, or, in the case of strongly magnetized plasmas, the cyclotron resonance, $\omega - k_{||}v_{||} - n\Omega_c/\gamma = 0$ (n = ±1, ±2, …).

An estimate of the theoretical current drive efficiency is obtained from the following arguments. Suppose the parallel momentum imparted to an electron is $m\Delta v_{||}$. The incremental current carried by this electron is $\Delta j = -e\Delta v_{||}$, while its incremental energy is $\Delta\varepsilon = mv_{||}\Delta v_{||}$. The fact that $\Delta\varepsilon/\Delta j$ is proportional to $v_{||}$, shows that it is energetically favorable to accelerate low parallel velocity electrons and, consequently, first studies of RF current drive focused on waves with low phase velocity $\omega/k \ll v_{te}$ such as Alfvén waves. However, the incremental current will decay with the collision frequency $\nu(v) \sim 1/v^3$ and the power required to sustain this current consequently is $P_{RF} = \nu(v)\Delta\varepsilon$. Using the notation $J = \Delta j$, and combining the expressions for Δj, $\Delta\varepsilon$ and P_{RF}, one obtains the theoretical steady state current drive efficiency as

$$\frac{J}{P_{RF}} = \frac{-e}{mv_{||}\nu(v)}. \tag{4}$$

Thus, maximizing the current drive efficiency requires minimizing the expression $v_{||}\nu(v)$. Optimization is obtained in two opposite limits (see also Fig. 1): for $v_{||} \to 0$, but $v_\perp \approx v_{te}$, one has $\nu(v) \approx$ constant; while for $v_{||} \gg v_{te}$, $\nu(v) \sim 1/v_{||}^3$. The second limit calls for the use of waves with high parallel phase velocity such as Lower Hybrid (LH) waves (lower hybrid current drive, LHCD).

It can be shown that the direct transfer of parallel momentum is not even a strict requirement for current drive. This was first realized by N.J. Fisch and A.H. Boozer [12]. The basic argument runs as follows. Take an electron with given parallel and perpendicular momentum, $m\boldsymbol{v}_1$. This electron would lose its parallel momentum in a typical momentum loss time defined by the collision frequency ν_1. As its parallel momentum decays, it would contribute a parallel current which averaged over the time Δt can be approximated by $J_1 \approx -ev_{||1}/\Delta t\,\nu_1$. Now, assume that after interaction with EC waves its momentum is changed by a small amount to $m\boldsymbol{v}_2$. Again it will lose its parallel momentum in a collision time, but the collision frequency is now changed since it is proportional to $1/v^3$. As a result a net current is generated, which can be equated to

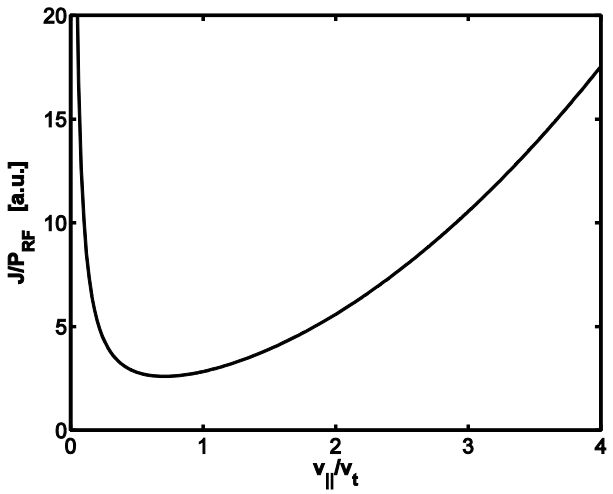

Figure 1: *The theoretical current drive efficiency (in arbitrary units) for direct momentum transfer as a function of the parallel velocity.*

$$J \equiv J_2 - J_1 \approx \frac{-e}{\Delta t}\left(\frac{v_{||2}}{\nu_2} - \frac{v_{||1}}{\nu_1} \right). \tag{5}$$

The power that has been spent to create this current is $(E_2 - E_1)/\Delta t$. Substituting differentials for the finite differences, this leads to the Fisch-Boozer current drive efficiency given by [6, 12]

$$\frac{J}{P_{RF}} = -e\frac{\hat{\boldsymbol{s}}\cdot\nabla_{\mathbf{p}}(v_{||}/\nu)}{\hat{\boldsymbol{s}}\cdot\nabla_{\mathbf{p}}(p^2/2m_e)} \tag{6}$$

where $\hat{\boldsymbol{s}}$ is the unit vector in the direction of RF driven momentum displacement. As parallel momentum transfer between waves and particles no longer is a requirement, also waves which carry little or no parallel momentum can be used for effective current drive. In fact, the theoretical efficiency for current drive by perpendicular pushing of electrons reaches up to 3/4 of the efficiency for direct parallel pushing of electrons [13]. This holds, in particular, for electron cyclotron current drive (ECCD).

It has subsequently been found that 'adjoint techniques' allow to find a more precise expression for the 'current response function', $\chi = -ev_{||}/\nu$. Starting from the steady state Fokker-Planck equation,

$$C(f_e(\boldsymbol{v})) = \nabla_{\mathrm{p}}\cdot\boldsymbol{S}_{\mathrm{w}}, \tag{7}$$

where $\boldsymbol{S}_w$ is the quasi-linear wave driven momentum space flux, an adjoint equation for the current response function can be written as [6, 14]

$$C(f_{em}(v)\chi(\boldsymbol{v})) = ev_{||}f_{em}(v), \quad (8)$$

where $f_{em}(v)$ is the Maxwellian distribution function, and $f_{em}(v)\chi(\boldsymbol{v})$ is required to have zero density and energy. Now, writing the current from the solution to the steady state Fokker-Planck equation as

$$J = -\int ev_{||} f_e(\boldsymbol{v})\, d^3v = -\int (f_e/f_{em})\, C(f_{em}\chi)\, d^3v, \quad (9)$$

and using the self-adjointness of the collision operator,

$$\int \psi\, C(f_{em}\chi)\, d^3v = \int \chi\, C(f_{em}\psi)\, d^3v, \quad (10)$$

it is easily shown that

$$J = \int \boldsymbol{S}_w \cdot \nabla_p \chi\, d^3v. \quad (11)$$

The current drive efficiency then becomes

$$\frac{J}{P_{RF}} = -e\frac{\int \hat{\boldsymbol{s}} \cdot \nabla_{\mathbf{p}} \chi d^3v}{\int \hat{\boldsymbol{s}} \cdot \nabla_{\mathbf{p}} (p^2/2m_e) d^3v} \quad (12)$$

generalizing the Fisch-Boozer efficiency (6). These adjoint techniques are limited to the regime in which the plasma response to the RF waves is almost linear. When significant quasi-linear modifications of the distribution function are induced, a proper estimate of the driven current can only be obtained from solution of the full Fokker-Planck equation.

The presence of trapped electrons further complicates the picture: in a tokamak or stellarator, all particles in the cone in velocity space given by $|v_{||0}/v_{\perp 0}| < (B_{max}/B_{min}-1)^{0.5}$ are trapped between the magnetic field maxima along a field line [2]. Trapped particles have zero average parallel velocity and cannot contribute to the parallel current. Consequently, when a passing particle crosses the trapped/ passing boundary during its slowing down, it no longer contributes any parallel current. This will reduce the current drive efficiency. As a passing particle is pushed across the trapped/passing boundary by the resonant interaction with RF waves, its contribution to the parallel current is lost and a net current is driven in the opposite direction, which is known as the Ohkawa current [15]. Furthermore, increasing a particle's perpendicular energy near the maximum in the magnetic field will increase its parallel velocity on the remainder of its trajectory. This should favor current drive by pushing particles in the perpendicular direction (in particular, ECCD) on the high field side. All these effects can be included in an adjoint calculation of the current drive efficiency by calculating the appropriate current response function for the bounce-averaged Fokker-Planck equation [16, 17, 18].

III.A. Lower Hybrid Current Drive (LHCD)

LHCD has proven to be the most successful non-inductive current drive method in tokamaks to date [19]. It makes use of the slow wave in the intermediate frequency regime between the ion and electron cyclotron frequencies: $\Omega_{ci} \ll \omega \ll |\Omega_{ce}|$. This is the realm of the lower hybrid resonance,

$$\omega_{LH} = \frac{\omega_{pi}^2}{1+\omega_{pe}^2/\Omega_{ce}^2} = \frac{|\Omega_{ci}\Omega_{ce}|}{1+\Omega_{ce}^2/\omega_{pe}^2}. \quad (13)$$

For the slow wave to have access to the high density part of the plasma in this frequency range, the parallel refractive index must satisfy the accessibility condition [20]

$$N_{||} > N_c \equiv \frac{1}{1-\omega^2/|\Omega_{ci}\Omega_{ce}|}. \quad (14)$$

As a result, the waves are evanescent at the plasma edge and efficient coupling of the waves requires a close proximity of the LH wave antenna to the plasma edge. A particular property of lower hybrid waves is that the group velocity is perpendicular to the wave vector. Since also typically $k_\perp \gg k_{||}$, the group velocity is almost parallel to the magnetic field and the wave propagates in a narrow "resonance cone" along the magnetic field. This means that the waves can only reach the centre of the plasma after traveling a number of times around the torus.

For efficient current drive, one should avoid parasitic damping of the waves by ions and, in case of a reactor, by fusion alpha particles. This requires the use of sufficiently high frequencies in order to avoid the presence of the lower hybrid resonance inside the plasma. In addition, efficient current drive is favored by high phase velocities, i.e. small $N_{||}$. While one would expect such high phase velocities with $v_{ph} \gg v_{te}$ to be ill absorbed as a consequence of exponentially small numbers of resonant electrons, early experiments nevertheless showed good absorption. The reason for this is the generation of an extended tail of energetic electrons by quasi-linear interaction with lower phase velocity components not originally present in the launched wave spectrum. The generation in the plasma of these lower phase velocity components is known as the "spectral gap" problem. It is generally assumed that the multi-pass ray trajectories in these experiments are responsible for the required $N_{||}$ upshift [21]. Several alternative explanations have been proposed to fill the spectral gap, including spectral broadening due to scattering off density fluctuations, wave diffraction, magnetic ripple, and parametric instabilities in the scrape-off layer in front of the launching antenna [22]. State of the art modeling employs coupled 3D ray-tracing and (2D in velocity space) Fokker-Planck codes with self-consistent absorption from the quasi-linearly modified electron distribution function [23]. This standard model of LHCD has proven very successful in explaining present experimental results [24].

LHCD has been the main tool for bulk current drive and for current profile tailoring in reversed central shear or low shear, hybrid tokamak scenarios. A record 3 hour discharge sustained by LHCD has been demonstrated on TRIAM-1M albeit at low current and density. On larger devices like JET and JT-60 fully non-inductive discharges have been sustained by LHCD at 3.0 and 3.6 MA, respectively. Current drive efficiencies obtained to date have reached values of $\eta_{LHCD} = 0.3\times10^{20}$ A/Wm^2

(JT-60U and JET), and across different experiments are found to scale roughly as $\eta_{LHCD} \approx 1.2 \times 10^{20} <T_e[keV]> / (5+Z_{eff})$ A/Wm^2 [8].

In ITER, the penetration of LH waves is limited to the outer parts as very efficient Landau damping occurs at plasma temperatures in the range of ~10 keV. Simulations confirm this limitation of LHCD to the colder outer part of the plasma. Typical efficiencies predicted for ITER are in the range of $\eta_{LHCD} = 0.2 \times 10^{20}$ A/Wm^2 [23]. The major aim of a possible LHCD system for ITER would be the achievement and sustainment of reversed shear or hybrid tokamak scenarios and the generation of discharges with fully non-inductive current drive.

Typical frequencies used for LHCD are in the range of 1 to 10 GHz, and in this frequency range fundamental wave guides can be used for an efficient transport of the waves. To generate the required spectrum grill antennae existing of multiple, appropriately phased fundamental wave guides are being used [20]. Also high power sources in this frequency range, especially klystrons, are readily available.

III.B. Electron Cyclotron Current Drive (ECCD)

Electron cyclotron waves generally carry little or no momentum, and current drive by these waves is based on the Fisch-Boozer mechanism in which electrons moving in one direction are selectively heated [25, 26]. This selective heating can be achieved by proper tailoring of the EC resonance condition,

$$\omega = n \mid \Omega_{ce} \mid / \gamma + k_{||} v_{||} \qquad (15)$$

in the region of power deposition. It generally requires a finite parallel refractive index, $N_{||} = k_{||}c/\omega$, and sufficient optical depth in order to guarantee almost complete absorption on one side of the resonance. One then distinguishes ECCD at downshifted ($\omega < |\Omega_{ce}|$) and at upshifted frequencies ($\omega > |\Omega_{ce}|$) as illustrated in Fig. 2. Efficient downshifted ECCD can be obtained by oblique injection of slow X-mode waves at the fundamental resonance from the high field side. However, most experiments currently affect ECCD at upshifted frequencies by low field side oblique injection of either fundamental O-mode or second harmonic fast X-mode waves. State of the art modeling of ECCD employs ray- or beam tracing codes employing adjoint techniques for the calculation of the driven current [27]. Quasi-linear modifications of the electron distribution become significant for power levels exceeding the threshold value $p_{ECCD}[MW/m^3]/n_e^2[10^{19}/m^3] > 0.5$ [28]. In such cases proper predictions of the EC driven current can only be obtained from (2D in velocity space) bounce averaged quasi-linear Fokker-Planck codes [29].

The current drive figures of merit achieved to date are typically in the range of $\eta_{ECCD} = 1 - 4 \times 10^{18}$ A/Wm^2, where the largest values have been achieved in high temperature discharges on JT-60U [30]. Extensive studies on DIII-D have shown that the experimentally measured EC driven current is in good agreement with predictions from combined ray-tracing and Fokker-

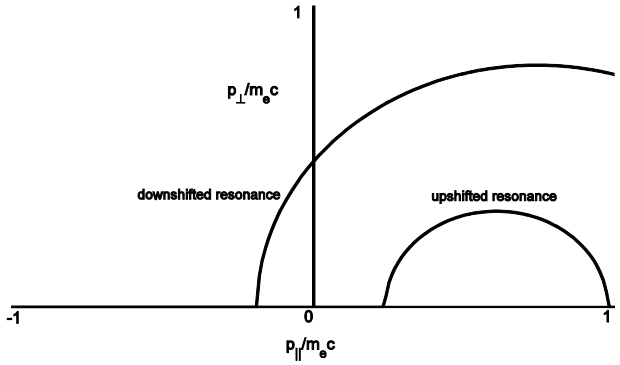

Figure 2: *Illustration of the down and up shifted EC resonance in momentum space. The parallel refractive index is $N_{||} = 0.5$, and the wave frequencies are chosen as $\omega / |\Omega_{ce}| = 0.9$ and 1.1 for the down- and upshifted case, respectively.*

Planck code calculations provided the synergy between the ECCD and a residual parallel electric field is properly accounted for [31]. Full non-inductive current drive over several current diffusion times has been demonstrated on TCV [32]. In these discharges, the EC driven current density profile had to be carefully tailored in order to avoid driving too much current near the centre of the discharge and the resulting instabilities. This is a due to the very localized EC power absorption and current drive as a consequence of the use of well focused wave beams and the cyclotron resonant character of the wave-plasma interaction. This localized character of the ECCD is in fact its main attractive feature: it allows the localized manipulation of the current density profile as required for the control of MHD instabilities like sawteeth and neoclassical tearing modes [25, 26].

Calculations of the expected ECCD efficiency in ITER predict a value of $\eta_{ECCD} = 0.2 \times 10^{20}$ A/Wm^2 in the high temperature centre of the discharge. Off-axis ECCD efficiencies will be significantly lower as a consequence of both trapped particle effects and lower local temperatures. Still the predicted driven current densities for the total available power of 20 MW are more than sufficient for the control of sawteeth and tearing modes [33], one of the major tasks of the ITER ECRH system.

III.C. Ion cyclotron resonance frequency (ICRF)

Current drive by ICRF waves (ICCD) is possible in a variety of scenarios [7, 8]. The wave to be injected in this range of frequencies is the fast magnetosonic wave (or fast wave FW), which has a dominant perpendicular electric field polarization [34]. Avoiding significant damping on the ions or mode conversion to ion Bernstein waves, most of the power can be deposited on electrons through multi pass absorption by electron Landau-damping and transit time magnetic pumping (TTMP). In case of the injection of an asymmetric wave spectrum, these result in fast wave current drive (FWCD). FWCD has been demonstrated on JFT-2M, DIII-D [35], and Tore-Supra [36]. Current drive efficiencies obtained scale with the central electron

temperature and have reached values up to $\eta_{FWCD} = 4 \times 10^{18}$ A/Wm^2 in agreement with theoretical modeling [7, 37]. Typical driven current density profiles are very peaked on axis due to both central peaking of the power deposition and trapped particle effects. Extrapolation of these results to ITER yield an expected current drive efficiency of $\eta_{FWCD} = 0.2 \times 10^{20}$ A/Wm^2 with a centrally peaked driven current density profile.

Alternative scenarios of ICCD make use of the generation of extended energetic ion tails, for example, through ion minority heating. In the case of asymmetric wave particle interaction, these can result in a sizeable driven ion current, which can be calculated from a trivial generalization of the Fisch-Boozer efficiency (6). As in the case of Neutral Beam current drive (see section IV) this energetic ion current J_m (with minority ion charge Z_m) results in a net plasma current $J = J_m (1 - Z_m/Z_i)$ where Z_i is the majority ion charge. The final equation for the ion minority current drive efficiency then becomes [6]

$$\frac{J}{P_{ICCD}} = eZ_m(1 - Z_m/Z_i)\frac{\hat{\boldsymbol{s}}\cdot\nabla_{\mathbf{p}} v_{\|}/\nu}{\hat{\boldsymbol{s}}\cdot\nabla_{\mathbf{p}} p^2/2m_e}. \qquad (16)$$

Additional energetic ion currents can arise from finite orbit widths of (trapped) resonant ions [38]. These latter currents are highly localized and due to their diamagnetic origin typically of bipolar shape. This makes these currents well suited for MHD instability control. Successful control of sawteeth has been demonstrated by ICCD on JET resulting in possible avoidance of NTM [39].

III.D. Alfvén wave Current Drive (AWCD)

At first glance, current drive by low frequency $\omega < \Omega_{ci}$, low phase velocity $v_{ph} < v_{te}$ Alfvén waves appears very attractive as the current drive efficiency increases dramatically for low phase velocities (see Fig. 1). However, as the wave momentum is imparted to electrons with very small parallel velocity, most of these electrons are likely to be trapped. For this reason efficiencies for AWCD are expected to be very low. In one of the few experiments an efficiency of $\eta_{AWCD} = 0.4 \times 10^{18}$ A/Wm^2 was achieved. However, the favorable regime with very low phase velocity $v_{ph} < v_{te}$ could not be accessed [40].

IV. NEUTRAL BEAM CURRENT DRIVE (NBCD)

The possibility of current drive by the injection of energetic beams of neutral particles was already realized in the early stages of tokamak research [41]. Following the discussion as given in Ref. [6], the principle of NBCD can be understood as follows. Consider a homogeneous, neutral plasma with two groups of counter streaming ions. It is then always possible to choose the frame of reference such that their currents cancel exactly and the net ion current vanishes. When one of the two ion populations, say the left moving bulk ions, can now be made to collide more efficiently with the electrons then the right moving beam ions, the

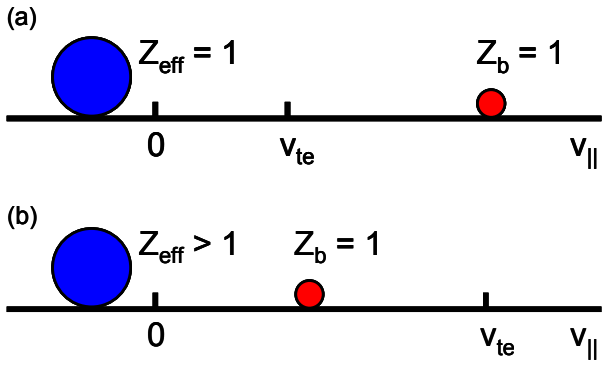

Figure 3: *Illustration of the principle of neutral beam current drive. A difference in the momentum transfer rate from bulk (left) and beam (right) ions to the electrons is due to (a) a beam velocity well in excess of the electron thermal velocity or (b) a difference in charge state between bulk and beam ions.*

electrons will be displaced in the direction of this left moving bulk ions and a net plasma current in the opposite direction would result. Finally, note that in neutral plasma the current is a Lorentz invariant, such that it is independent of the frame of reference in which it is derived.

Two possible ways to realize such a situation with different momentum transfer rates from the bulk and beam ion populations to the electrons are sketched in Fig. 3 (after Ref. [6]). In the first example (Fig. 3a), a beam of highly energetic ions is moving to the right at velocities v_b well above the electron thermal velocity (i.e. $v_b \gg v_{te}$). Due to the velocity dependence of the Coulomb collision frequency, the electrons would then collide much more frequently with the left moving bulk ion population, and a net current to the right would result. As said, this requires neutral beam injection with beam velocity far exceeding the electron thermal velocity, which in high temperature fusion plasmas is unpractical.

In the second example (Fig. 3b), the beam velocity maybe smaller than the electron thermal velocity (i.e. $v_b < v_{te}$). A difference in momentum transfer rates is now obtained by exploiting the dependence of the Coulomb collision frequency on the square of the ion charge state Z_i, while the current carried is only linear in Z_i. When the effective charge state of the bulk ions Z_{eff} now exceeds that of the energetic ion beam Z_b (or vice versa), the electrons again will collide more frequently with the left moving bulk ions (the beam ions), and a net current to the right (left) will arise. Neglecting trapped electron effects, this results in a current

$$J = \left(1 - \frac{Z_b}{Z_{eff}}\right) J_b, \qquad (17)$$

where J_b is the current carried by the energetic ion beam. Trapped electron effects further restrain the electron motion, resulting in a further reduction of the cancelling electron current. In the large aspect ratio approximation the net result is [9,42]

$$J = \left(1 - \frac{Z_b}{Z_{eff}}\left(1 - 1.46\sqrt{\varepsilon}\,A(Z_{eff})\right)\right) J_b\,, \qquad (18)$$

where $A(Z_{\rm eff})$ is a function whose values vary from 1.67 for $Z_{\rm eff} = 1$ to 1.18 for $Z_{\rm eff} = 4$.

A calculation of the beam current J_b, requires a Fokker-Planck solution of the beam ion distribution. In the absence of trapping an analytical solution for this 'slowing down distribution' has been found in the form [9]

$$J_b = p_{NBCD} \frac{2\tau_s e Z_b}{m_b v_b (1 + u_c^2)} \int_0^1 f_1(u) u^3 du \qquad (19)$$

where $p_{\rm NBCD}$ is the local density of neutral beam power deposition, $m_{\rm b}$ the mass of the beam ions, $\tau_{\rm s}$ is the energetic ion slowing down time, and u is the energetic ion velocity normalized to the injection velocity $v_{\rm b}$. The function f_1 is the first order Legendre harmonic of the energetic ion distribution function, and is given by

$$f_1(u) = u^{2\beta} \left(\frac{1 + u_c^3}{u^3 + u_c^3}\right)^{1+2\beta/3}\,, \qquad (20)$$

where

$$\beta = \frac{m_i Z_{eff}}{2 m_b \overline{Z}}\,, \qquad u_c^3 = \frac{3\sqrt{\pi} m_e \overline{Z} v_{te}^3}{4 m_i v_b^3}$$

and

$$\overline{Z} = \sum_i \frac{m_b n_i Z_i^2}{m_i n_e}$$

where the subscript i refers to the different bulk ion species.

NBCD has been applied successfully in a number of tokamaks. The maximum driven currents are in agreement with the theoretical expectations according to the model outlined above [8]. Typical beam energies in current experiments range from several 10's of keV in the smaller tokamaks up to 350 keV in the larger JT-60U tokamak. For efficient penetration into the high density ITER core, beam energies of 0.5 to 1 MeV will be required. The efficient neutralization of the accelerated beam ions before injection into the plasma at these high energies is only possible using negative ion sources. Due to the nature of the NB power deposition the NBCD profile can be relatively broad, and is most useful for driving bulk plasma current rather than current density profile tailoring. A record NBCD efficiency of $\eta_{\rm NBCD} = 0.15 \times 10^{20}$ A/Wm^2 has been achieved on JT-60U using negative ion based NBCD at beam energies of 350 keV in $T_e(0) = 14$ keV, high beta plasmas with fully non-inductive plasma current sustainment [43]. Calculations for ITER conditions predict NBCD efficiencies up to $\eta_{\rm NBCD} = 0.4 \times 10^{20}$ A/Wm^2 [7] for an optimized system.

V. ALTERNATIVE METHODS

Many alternative methods have been considered in the literature. However, none of these methods has achieved the experimental maturity of the RF and neutral beam based current drive methods discussed above. We will provide only a cursory sketch of these alternatives.

V.A. Helicity injection

Helicity is defined as the inner product of the vector potential and the magnetic field, $K \equiv \boldsymbol{A}\cdot\boldsymbol{B}$, where the vector potential $\boldsymbol{A}$ satisfies $\boldsymbol{B} = \nabla\times\boldsymbol{A}$. A transport equation for helicity can be written using Ohm's law as [44]

$$\frac{\partial K}{\partial t} + \boldsymbol{\nabla}\cdot\boldsymbol{Q} = -2\eta \boldsymbol{J}\cdot\boldsymbol{B}, \qquad (21)$$

where the helicity flux is

$$\boldsymbol{Q} = \boldsymbol{B}\phi + \boldsymbol{E}\times\boldsymbol{A} = 2\boldsymbol{B}\phi + \boldsymbol{A}\times\partial\boldsymbol{A}/\partial t \qquad (22)$$

with ϕ being the electrostatic potential, and the total electric field $\boldsymbol{E} = -\boldsymbol{\nabla}\phi - \partial\boldsymbol{A}/\partial t$. The evolution of the total magnetic helicity $K_{\rm tot} \equiv \int \boldsymbol{A}\cdot\boldsymbol{B}\,{\rm d}V$, where the integration is over a plasma volume bounded by a magnetic surface, then is given by

$$\frac{\partial K_{tot}}{\partial t} = 2V_{loop}\Phi_T - \int 2\,\eta\,\boldsymbol{J}\cdot\boldsymbol{B}{\rm d}V. \qquad (23)$$

Here, the first term on the right hand side represents the helicity injection at the edge of the plasma given by the product of the toroidal loop voltage and the toroidal magnetic flux. The second term represents the volume integrated helicity dissipation. In the case of inductive current drive the dissipation of helicity is canceled by a DC loop voltage, which is limited by the flux swing of the primary transformer. In the concept of oscillating field current drive (OFCD) (or AC helicity injection) very low frequency, oscillating toroidal and poloidal electric fields are applied at the plasma edge, with relative phasing such that net time averaged helicity injection is obtained [45, 46]. The current generated in this way is located at the plasma surface and penetration to the plasma core must rely on Taylor relaxation: the conjecture that magnetically confined plasmas tend to relax to states with minimum magnetic energy while conserving total helicity [47]. An experimental demonstration is given in Ref. [48].

Electrostatic (or DC) helicity injection makes use of the term $2\boldsymbol{B}\phi$ in the helicity flux (22). This is only possible in case of open field lines exciting and entering the plasma volume. A simple prescription for electrostatic helicity injection then would be to cut an electric gap dividing the bounding surface into two areas where magnetic flux either enters or leaves the volume and to apply a voltage V over this electric gap. This results in an amount of helicity injection given by [44]

$$\left.\frac{\partial K_{tot}}{\partial t}\right|_{inj} = 2V\Phi_M\,, \qquad (24)$$

where

$$\Phi_M = \frac{1}{2}\int |\boldsymbol{B}\cdot\boldsymbol{n}|\,{\rm d}S$$

is the net flux entering/leaving the volume. The method has been applied successfully in a number of experiments using different geometries for the applied magnetic fields and voltages [49–52], and appears

particularly useful for current start-up in solenoid-free spherical tokamaks [53].

V.B. Alpha power channeling

The basic idea of 'alpha power channeling' is to transfer energy from the energetic fusion alpha particles into waves, which may then be put to practical use. The transfer of energy from particles to waves requires the inversion of the alpha particle distribution along the wave diffusion trajectory. In the original proposal, the alpha particle energy is channeled through interaction with Lower Hybrid waves into current drive [54]. Later, alpha particle interaction with Ion Bernstein waves has been envisaged to channel alpha particle energy into heating of fuel ions with the potential of increasing the plasma reactivity [55]. A review of the main concepts and of some partial experimental tests is given in Ref. [56].

V.C. Synchrotron radiation

Fusion plasmas are a powerful source of synchrotron radiation. As the tokamak vessel walls are generally highly reflective for these waves, the radiation is continuously emitted and reabsorbed. Whereas the emitted radiation is isotropic, it has been suggested that by proper shaping of the vessel walls the reflected spectrum can be made anisotropic such that the reflected waves could effectively drive plasma current [57]. The anisotropic reflection is achieved by means of a sawtoothed or fish-scale wall in which the vertical sections are made absorbing while the slanted sections are made reflecting. Further investigations seem to indicate that only part of the current can be driven in this way in a realistic fusion reactor [58, 59].

VI. SYNERGY

So far, the different current drive schemes have been treated individually. Synergy could be expected from combinations of any of these. For example, combining LHCD and ECCD has been shown to significantly increase the ECCD efficiency as the EC waves can interact with the LHCD produced high energy tail electrons [60]. In another experiment the combination of LHCD and ion Bernstein waves (IBW) has been shown to lead to a locally increased LHCD current, which is due to the local generation of a broadened electron velocity distribution by the IBW on which the LHCD wave are damped more efficiently [61]. On JET a synergy between LHCD and the FWCD was noted [62]. An increased NBCD efficiency could be expected from ion cyclotron resonance heating of the energetic beam ions: the increase of the perpendicular velocity of the beam ions increases their slowing down time and the resulting beam current [63]. Finally, radial gradients in RF driven quasi-linear populations will affect the bootstrap current [64].

VII. PROSPECTS FOR A STEADY STATE TOKAMAK REACTOR

Even with the highest predicted current drive efficiencies quoted above, full non-inductive drive of the total plasma current in a standard high performance H-mode discharge in ITER would require a prohibitively large amount of power. As we can foresee now, the fully non-inductive, steady state operation of ITER and future tokamak fusion reactors will have to rely on the bootstrap current for supplying the major part of the plasma current. Other methods, like NBCD or ECCD, need than be used to supply sufficient core current to fill in the hollow bootstrap current profile $\sim\sqrt{\varepsilon}dp/dr$ [8]. Maximizing simultaneously bootstrap current fraction and performance is one of the goals of advanced tokamak scenario development. Integrated modeling of such scenarios illustrates the possibilities for steady state discharges in ITER [65].

ACKNOWLEDGMENTS

This work was carried out with financial support from NWO.

REFERENCES

[1] M. VAN SCHOOR, 'Fusion Machines', these proceedings.
[2] H.J. DE BLANK, 'Guiding centre orbits', these proceedings.
[3] D.A. HARTMANN, 'Stellarators', these proceedings.
[4] H.J. DE BLANK, 'MHD instabilities in tokamaks', these proceedings.
[5] H.R. KOSLOWSKI, 'Operational limits and limiting instabilities in tokamak machines', these proceedings.
[6] N.J. FISCH, Rev. Modern Phys. **59** 175 (1987).
[7] ITER Physics Basis, Chapter 6: Nucl. Fusion **39** 2495 (1999).
[8] C. GORMEZANO, et al, Nucl. Fusion **47** S285 (2007).
[9] J. WESSON, 'Tokamaks' Third Edition, (2004).
[10] P. HELANDER, 'Neoclassical transport in plasmas', these proceedings.
[11] A.G. PEETERS, Plasma Phys. Control. Fusion **42** B231 (2000).
[12] N.J. FISCH, A.H. BOOZER, Phys. Rev. Lett. **45** 720 (1980).
[13] C.F.F. KARNEY, N.J. FISCH, Nucl. Fusion **21**, 1549 (1981).
[14] C.F.F. KARNEY, Comp. Phys. Reports **4**, 183 (1986).
[15] T. OHKAWA, General Atomics Report GA-A13847 (1976).
[16] R.H. COHEN, Phys. Fluids **30**, 2442 (1987)
[17] Y.R. LIN-LIU, et al, Phys. Plasmas **10**, 4064 (2003).

[18] N.B. MARUSHCHENKO, et al, Nucl. Fusion **48**, 054002 (2008).
[19] Y. PEYSSON, in Radio Frequency Power in Plasmas, AIP Conf. Proc. **485**, 183 (1999).
[20] R.A. CAIRNS, Radiofrequency heating of plasmas, IOP Publishing, Bristol (1991).
[21] P.T. BONOLI, R.C. ENGLADE, Phys. Fluids **29**, 2937 (1986).
[22] R. CESARIO, et al, Nucl. Fusion **46**, 462 (2006).
[23] P.T. BONOLI, et al, in Radio Frequency Power in Plasmas, AIP Conf. Proc. **694**, 24 (2003).
[24] P.T. BONOLI, et al, Phys. Plasmas **15**, 056117 (2008).
[25] E. WESTERHOF, 'Electron Cyclotron Waves', these proceedings.
[26] R. PRATER, Phys. Plasmas **11**, 2349 (2004).
[27] R. PRATER, et al, Nucl. Fusion **48** 035006 (2008).
[28] R.W. HARVEY, et al, Phys. Rev. Lett. **62**, 426 (1989).
[29] E. WESTERHOF, 9th Joint Workshop on ECE and ECH, Borrego Springs, California, 1995, Ed. J. Lohr, World Scientific, Singapore, p. 3 (1995).
[30] T. SUZUKI, et al, Nucl. Fusion **44**, 699 (2004).
[31] C.C. PETTY, et al, Nucl. Fusion **42**, 1366 (2002).
[32] O. SAUTER, et al, Phys. Rev. Lett. **84**, 3322 (2000).
[33] G. RAMPONI, et al, Fusion Sci. Technol. **52** 193 (2007).
[34] F. LOUCHE, 'Coupling of EM waves to the plasma', these proceedings.
[35] R. PRATER, et al, Plasma Phys. Control. Fusion **35**, A53 (1993).
[36] EQUIPE TORE SUPRA, presented by B. Saoutic, Plasma Phys. Control. Fusion **36** B123 (1994).
[37] C.C. PETTY, et al, Plasma Phys. Control. Fusion **43** 1747 (2001).
[38] T. HELLSTEN, et al, Phys. Rev. Lett. **74** 3612 (1995).
[39] O. SAUTER, et al, Phys. Rev. Letters **88**, 105001 (2002).
[40] T. INTRATOR, et al, Phys. Plasmas **2**, 2263 (1995)
[41] T. OHKAWA, Nucl. Fusion **10**, 185 (1970).
[42] J.W. CONNER, J.G. CORDEY, Nucl. Fusion **14**, 185 (1974).
[43] T. OIKAWA, et al, Nucl. Fusion **41**, 1575 (2001).
[44] T.H. JENSSEN, M.S. CHU, Phys. Fluids **27**, 2881 (1984).
[45] P.M. BELLAN, Phys. Rev. Letters **54**, 1381 (1985).
[46] A.H. BOOZER, Phys. Fluids **29**, 4123 (1986).
[47] J.B. TAYLOR, Phys. Rev. Letters **33**, 1139 (1974).
[48] K.J. McCOLLAM, et al, Phys. Rev. Letters **96**, 035003 (2006).
[49] M. Ono, et al, Phys. Rev. Letters **59**, 2165 (1987).
[50] B.A. NELSON, et al, Phys. Plasmas **2**, 2337 (1995).
[51] A.J. REDD, et al, Phys. Plasmas **9**, 2006 (2002).
[52] R. RAMAN, et al, Nucl. Fusion **41**, 1081 (2001).
[53] R. RAMAN, et al, Nucl. Fusion **47**, 792 (2007).
[54] N.J. FISCH, J.M. RAX, Phys. Rev. Letters **69**, 612 (1992).
[55] N.J. FISCH, et al, Nucl. Fusion **34**, 1541 (1994).
[56] N.J. FISCH, Nucl. Fusion **40**, 1095 (200).
[57] J.M. DAWSON, P.K. KAW, Phys. Rev. Letters **48**, 1730 (1982).
[58] I. FIDONE, et al, Phys. Fluids **31**, 2300 (1988).
[59] W. KERNBICHLER, S.V. KASILOV, Phys. Plasmas **3**, 4128 (1996).
[60] G. GIRUZZI, et al, Phys. Rev. Letters **93**, 255002 (2004).
[61] F. PAOLETTI, et al, Phys. Plasmas **6**, 863 (1999).
[62] J. JACQUINOT, Plasma Phys. Control. Fusion **35**, A35 (1993).
[63] K. OKANO, et al, Nucl. Fusion **23**, 235 (1983).
[64] R.W. HARVEY, and G. Taylor, Phys. Plasmas **12**, 052509 (2005).
[65] W.A. HOULBERG, et al, Nucl. Fusion **45**, 1309 (2005).